

## Ubp8 and SAGA Regulate Snf1 AMP Kinase Activity<sup>▽</sup>

Marenda A. Wilson,<sup>2,3,4</sup> Evangelia Koutelou,<sup>2,3,4</sup> Calley Hirsch,<sup>2,3,4</sup> Kadir Akdemir,<sup>1,2,3</sup>  
Andria Schibler,<sup>2,3,4</sup> Michelle Craig Barton,<sup>1,2,3</sup> and Sharon Y. R. Dent<sup>2,3,4\*</sup>

Department of Biochemistry and Molecular Biology,<sup>1</sup> Program in Genes and Development,<sup>2</sup> Center for  
Cancer Epigenetics,<sup>3</sup> and Department of Molecular Carcinogenesis,<sup>4</sup> Science Park, The University of  
Texas M. D. Anderson Cancer Center, 1515 Holcombe Blvd., Box 1000, Houston, Texas 77030

Received 23 November 2010/Returned for modification 4 January 2011/Accepted 12 May 2011

**Posttranslational modifications of histone proteins play important roles in the modulation of gene expression. The *Saccharomyces cerevisiae* (yeast) 2-MDa SAGA (Spt-Ada-Gcn5) complex, a well-studied multisubunit histone modifier, regulates gene expression through Gcn5-mediated histone acetylation and Ubp8-mediated histone deubiquitination. Using a proteomics approach, we determined that the SAGA complex also deubiquitinates nonhistone proteins, including Snf1, an AMP-activated kinase. Ubp8-mediated deubiquitination of Snf1 affects the stability and phosphorylation state of Snf1, thereby affecting Snf1 kinase activity. Others have reported that Gal83 is phosphorylated by Snf1, and we found that deletion of *UBP8* causes decreased phosphorylation of Gal83, which is consistent with the effects of Ubp8 loss on Snf1 kinase functions. Overall, our data indicate that SAGA modulates the posttranslational modifications of Snf1 in order to fine-tune gene expression levels.**

Ubiquitination of cellular targets regulates many biological processes, from intracellular trafficking to gene expression. Although ubiquitination by ubiquitin (Ub) ligases is widely studied, less is known about subsequent deubiquitination (DUB) of cellular substrates. The identification of genes coding 16 deubiquitinases in the *Saccharomyces cerevisiae* (yeast) genome and genes coding at least 60 deubiquitinases in the human genome suggests that not only is deubiquitination important but also that deubiquitination may also occur in a substrate-specific manner to regulate specific cellular processes. Despite the lack of knowledge of the targets of many of these deubiquitinases, it is known that some of these enzymes impact cellular growth and function (3, 21, 46). Overexpression of certain deubiquitinases is associated with progression of malignancy in neuroblastomas and a variety of carcinomas, indicating that these enzymes may be oncogenic (27, 31, 38).

USP22, a deubiquitinase associated with the SAGA histone acetyltransferase (HAT) complex, was identified as a member of an 11-gene “death-from-cancer” signature that serves as a predictor of treatment resistance, aggressive growth, and metastasis of human tumors when overexpressed (7, 8). The SAGA complex is highly conserved, and its functions are best characterized in yeast (4, 9, 17, 23, 35). In addition to acetylating histone H3 via the Gcn5 subunit, SAGA also proteolytically cleaves ubiquitin moieties from histone H2B via the Ubp8 subunit, which is an ortholog of USP22 (13, 47). Ubp8-mediated deubiquitination of histone H2B regulates the expression of target genes by modulating the level of histone H3 lysine 4 methylation, a mark that is associated with active transcription (13). In addition, Ubp8 facilitates the recruitment of the C-

terminal domain kinase (Ctk1) to target gene promoters via histone H2B deubiquitination, which facilitates the transition from transcription initiation to elongation (43).

Interestingly, recent studies indicate that the functions of USP22 extend beyond histone H2B, as it also deubiquitinates components of the shelterin complex, such as TRF1 (2). Deubiquitination of TRF1 regulates its stability, thereby affecting telomere maintenance. The SAGA complex then may regulate a wide variety of cellular processes that extend beyond alteration of chromatin structures.

To address the possibility that additional factors may be targets of Ubp8/USP22-mediated deubiquitination, we performed a proteomic screen in *Saccharomyces cerevisiae*. Here, we report that Ubp8 can deubiquitinate Snf1, a highly conserved AMP-activated serine/threonine protein kinase that serves as an energy sensor in the cell. Our data indicate that hyperubiquitination of Snf1 affects its stability as well as its phosphorylation status, which is known to affect Snf1 kinase activity (14, 24, 36). Together, our results suggest that SAGA functions as a master regulator of gene expression not only by altering chromatin structures but also by regulating the stability and activity of transcriptional modulators.

### MATERIALS AND METHODS

**Plasmids.** Plasmid pUb221 (a generous gift of Daniel Finley [44]) contains a 6×His-myc-ubiquitin construct under the control of the copper-inducible *CUP1* promoter, *TRP1* and *URA3* selectable markers, and a 2μm origin of replication. Plasmid pESC-LEU (Stratagene) contains a *LEU2* selectable marker, a 2μm origin of replication, and two multicloning sites downstream of the *GAL1* and *GAL10* yeast promoter. Each multicloning site allows the addition of either a myc or FLAG epitope-tagged gene of interest, respectively. Plasmid pMW10 is a derivative of pESC-LEU and contains a myc-tagged *UBP8* gene under the control of the *GAL1* promoter. Plasmid pMW18 is a derivative of pESC-LEU and contains a FLAG-tagged *SNF1* gene under the control of the *GAL10* promoter. Plasmid pMW22 is a derivative of pMW10 and contains a myc-tagged *UBP8* gene under the control of the *GAL1* promoter and a FLAG-tagged *SNF1* gene under the control of the *GAL10* promoter. Plasmid pRG145 (a generous gift of Richard Gardner), contains a three-hemagglutinin (3×HA)-tagged ubiq-

\* Corresponding author. Mailing address: Science Park, The University of Texas M. D. Anderson Cancer Center, 1515 Holcombe Blvd., Box 1000, Houston, TX 77030. Phone: (512) 237-9401. Fax: (512) 237-3439. E-mail: sroth@mdanderson.org.

<sup>▽</sup> Published ahead of print on 31 May 2011.

TABLE 1. *Saccharomyces cerevisiae* strains used in this study

Strain	Genotype	Source or reference
BY4741	<i>MATa his3Δ1 leu2Δ0 ura3Δ0 met15Δ0</i>	Open Biosystems
yMW16	<i>MATa his3Δ1 leu2Δ0 ura3Δ0 met15Δ0 ubp8Δ::KanMX6</i>	This study
YSC1178-7500067	<i>MATa his3Δ1 leu2Δ0 ura3Δ0 met15Δ0 SNF1-TAP::HIS3MX6</i>	Open Biosystems
yKL142	<i>MATa ura3-1 leu2-3,112 his3-11,15 trp1-1 ade2-1 htb1-1 htb2-1 pRS314 (FLAG-HTB1-CEN-TRP1) ubp8Δ::KanMX6 pRG145 (GAPDHP-3×HA-UBI4-URA3 integrative)</i>	18
YSC1178-7500046	<i>MATa his3Δ1 leu2Δ0 ura3Δ0 met15Δ0 ADA2-TAP::HIS3MX6</i>	Open Biosystems
yMW114	<i>MATa his3Δ1 leu2Δ0 ura3Δ0 met15Δ0 SNF1-TAP::HIS3MX6 ubp8Δ::KanMX6</i>	This study
yMW122	<i>MATa his3Δ1 leu2Δ0 ura3Δ0 met15Δ0 ADA2-TAP::HIS3MX6 ubp8Δ::KanMX6</i>	This study
YSC1178-7500191	<i>MATa his3Δ1 leu2Δ0 ura3Δ0 met15Δ0 GAL83-TAP::HIS3MX6</i>	Open Biosystems
YSC1021-555840	<i>MATa his3Δ1 leu2Δ0 ura3Δ0 met15Δ0 snf1Δ::KanMX6</i>	Open Biosystems
yMW129	<i>MATa his3Δ1 leu2Δ0 ura3Δ0 met15Δ0 GAL83-TAP::HIS3MX6 ubp8Δ::KanMX6</i>	This study
yMW134	<i>MATa his3Δ1 leu2Δ0 ura3Δ0 met15Δ0 GAL83-TAP::HIS3MX6 snf1Δ::KanMX6</i>	This study
YSC1178-7502243	<i>MATa his3Δ1 leu2Δ0 ura3Δ0 met15Δ0 UBP8-TAP::HIS3MX6</i>	Open Biosystems
yMW100	<i>MATa his3Δ1 leu2Δ0 ura3Δ0 met15Δ0 snf1Δ::KanMX6</i>	This study

uitin construct under the control of the *TDH3* promoter, a *URA3* selectable marker, and a 2μm origin of replication.

**Yeast transformations.** Yeast strains were transformed as previously described (Table 1) (6). To delete *UBP8* or *SNF1*, we PCR amplified the disrupted gene from a yeast deletion strain in the Open Biosystems collection (YSC1021-55154 or YSC1021-555840, respectively) by using primers that annealed 500 bp upstream and downstream of the indicated open reading frame (*UBP8* upstream primer oMW3, AACCTTTCCATTTCGCG; *UBP8* downstream primer oMW4, GCC AAAGACGGATATTTCTTGG) (*SNF1* upstream primer oMW136, AAAAGG ATGGGCGTGATGAT; *SNF1* downstream primer oMW137, GCAATGGGA GCAAAATTTCC). A one-step gene replacement was performed in the indicated strains by transformation using standard techniques (42). To confirm the deletion of either *UBP8* or *SNF1*, we PCR amplified G418-resistant colonies with primers that annealed within the KANMX6 cassette (KANC, TGATTTT GATGACGAGCGTAAT) and 700 bp downstream of the indicated open reading frame (*UBP8* downstream primer oMW140, CCGATGCAGAAAATGAAC TCGGTG; *SNF1* downstream primer oMW139, CTAACATCTGTCCAAAT GTTGG).

**Detection of hyperubiquitinated Snf1 in the absence of *UBP8*.** An analysis of Snf1 ubiquitination was performed under denaturing conditions with isogenic wild-type (YSC1178-750067) and *ubp8Δ* (yMW114) strains expressing a tandem affinity purification (TAP)-tagged version of Snf1 (Snf1-TAP) and copper-inducible 6×His-myc-ubiquitin construct as previously described but with modifications (37). Briefly, overnight cultures grown in 5 ml of synthetic complete medium minus uracil (SC-URA) plus 2% glucose were diluted in 50 ml of SC-URA plus 2% glucose to a starting optical density at 600 nm ( $OD_{600}$ ) of 0.2 and grown to an  $OD_{600}$  of 0.6 at 30°C. Twenty micromolar Z-Leu-Leu-Al (MG132; Sigma, St. Louis, MO) and 500 μM CuSO<sub>4</sub> were then added at final concentrations to each culture for 2 h, and cellular pellets were collected by centrifugation. Samples were lysed in 1 ml of cold buffer A (6 M guanidine-HCl, 0.1 M Na<sub>2</sub>HPO<sub>4</sub>/NaH<sub>2</sub>PO<sub>4</sub>, 10 mM imidazole, pH to 8.0). Clarified extracts were incubated with 50 μl of preequilibrated nickel-nitrilotriacetic acid (NTA) agarose beads (Qiagen, Valencia, CA) for 2 h and then washed 3 times for 10 min with buffer A. Next, samples were washed 3 times for 10 min in buffer A-buffer TI (1 volume of buffer A, 3 volumes of buffer TI [25 mM Tris-HCl, 20 mM imidazole, pH to 6.8]) and then once with buffer TI and boiled in 5× SDS-PAGE loading buffer containing 200 mM imidazole. Next, eluates were separated by SDS-PAGE, transferred to nitrocellulose membranes, and probed with anti-protein A antibodies (Molecular Probes, Eugene, OR) to detect Snf1-TAP.

In order to detect hyperubiquitination of the Snf1-FLAG construct in the absence of *UBP8*, 50-ml cultures of wild-type and *ubp8Δ* strains grown in synthetic complete medium minus leucine and uracil (SC-Leu-URA) plus 2% galactose and 2% sucrose in the presence of MG132 (see above) were lysed in 750 μl of IP300 buffer (50 mM Tris-HCl, pH 7.5, 300 mM NaCl, 2 mM MgCl<sub>2</sub>, 0.1% Triton X-100, 10% glycerol, 1 mM β-mercaptoethanol [β-ME], Complete protease inhibitors [Roche, Indianapolis, IN]). Snf1-FLAG was then purified from each lysate by using anti-FLAG agarose beads (Sigma, St. Louis, MO) in the presence of a deubiquitination (DUB) inhibitor (10 mM *N*-ethylmaleimide [NEM]) and MG132. Eluates were separated by SDS-PAGE and transferred to nitrocellulose membranes which were then probed with either anti-FLAG anti-

bodies (Sigma, St. Louis, MO) or anti-myc antibodies (Santa Cruz Biotechnologies, Santa Cruz, CA) to detect Snf1-FLAG and the 6×His-myc-Ub reporter, respectively.

**Coimmunoprecipitation of Ubp8 and Snf1.** BY4741 strains containing plasmid pESC-LEU, pMW10, pMW18, or pMW22 grown to a final  $OD_{600}$  of 0.8 in 50 ml of SC-Leu plus 2% galactose and 2% sucrose were lysed in 750 μl of IP300 buffer (50 mM Tris-HCl, pH 7.5, 300 mM NaCl, 2 mM MgCl<sub>2</sub>, 0.1% Triton X-100, 10% glycerol, 1 mM β-ME, Complete protease inhibitors [Roche, Indianapolis, IN]). Lysates were then preincubated with 200 units of DNase I for 1 h followed by a 3-h incubation with either 50 μl of preequilibrated anti-FLAG or anti-myc affinity resin (Sigma, St. Louis, MO) followed by three 10-min washes with 1 ml of IP300. Next, the beads were boiled in 5× SDS-PAGE loading buffer, and the proteins within the supernatant were separated by SDS-PAGE, transferred to nitrocellulose membranes, and probed with either anti-FLAG (Sigma, St. Louis, MO) or anti-myc (Santa Cruz Biotechnologies, Santa Cruz, CA) antibodies.

In order to determine if endogenous Snf1 and Ubp8 strains interact, YSC1178-7502243, BY4741, and yMW100 strains were grown to a final  $OD_{600}$  of 0.8 in 50 ml of yeast extract-peptone (YEP) plus 2% glucose and were lysed in 1 ml of IP300 buffer (50 mM Tris-HCl, pH 7.5, 300 mM NaCl, 2 mM MgCl<sub>2</sub>, 0.1% Triton X-100, 10% glycerol, 1 mM β-ME, Complete protease inhibitors [Roche, Indianapolis, IN]). Lysates were then preincubated with 200 units of DNase I for 1 h followed by a 4-h incubation with 40 μl of preequilibrated nickel-NTA agarose beads (Qiagen, Valencia, California) followed by three 10 min-washes with 1 ml of IP300. Next, the beads were boiled in 5× SDS-PAGE loading buffer, and the proteins within the supernatant were separated by SDS-PAGE, transferred to nitrocellulose membranes, and probed with either anti-6×His (Qiagen, Valencia, CA) or anti-protein A (Molecular Probes, Eugene, OR) antibodies.

**Isolation of the SAGA complex.** The SAGA complex was purified as previously described with modifications (18). Briefly, overnight cultures of YSC1178-7500046 and yMW122 were diluted into 12 liters of YEP plus 2% glucose to a starting  $OD_{600}$  of 0.2 and grown to a final  $OD_{600}$  of 0.8, collected by centrifugation, and resuspended in 150 ml of SAGA isolation buffer (40 mM HEPES, pH 7.4, 350 mM NaCl, 10% glycerol, 0.1% Tween 20 plus aprotinin [4 μg/ml], leupeptin [4 μg/ml], pepstatin [2 μg/ml], benzamidin [4 μg/ml], and phenylmethylsulfonyl fluoride [PMSF; 200 μg/ml]). Samples were lysed in a bead beater (Biospec) containing 150 ml of cold acid-washed glass beads with five 1-min beating cycles following by 5 min of cooling on ice. Clarified extracts were incubated with 500 μl of preequilibrated IgG sepharose (GE Healthcare, Piscataway, NJ) overnight and then washed twice with 10 ml of SAGA isolation buffer. Next, the beads were washed with 10 ml of TEV cleavage buffer (10 mM Tris-HCl, pH 8.0, 150 mM NaCl, 0.1% NP-40, 0.5 mM EDTA, 10% glycerol, 1 mM dithiothreitol [DTT] plus aprotinin [4 μg/ml], leupeptin [4 μg/ml], pepstatin [2 μg/ml], benzamidin [4 μg/ml], and phenylmethylsulfonyl fluoride [200 μg/ml]). The beads were then resuspended in 350 μl of TEV cleavage buffer containing 150 U of TEV protease (Invitrogen, Carlsbad, CA) overnight at 4°C. Eluates were collected, flash frozen in liquid nitrogen, and stored at −80°C.

**In vitro DUB assay.** Ubiquitinated H2B purified from yKL142 (kindly provided by Jerry Workman) or ubiquitinated Snf1 purified from yMW16 containing

pRG145 was incubated in DUB buffer (50 mM Na-HEPES, pH 7.5, 0.5 mM EDTA, 1 mM DTT, 0.1 M NaCl, 0.1 mg/ml ovalbumin) with SAGA complexes that were isolated from either YSC1178-7500046 or yMW122 strains. The reaction mixtures were incubated for 15 min at 30°C. SDS-PAGE loading buffer (5×) was added to each sample and boiled at 95°C for 5 min. Samples were separated by SDS-PAGE, transferred to nitrocellulose membranes, and subjected to a Western blot analysis with anti-FLAG antibodies (Sigma, St. Louis, MO), anti-HA antibodies (Roche, Indianapolis, IN), and anti-H2B antibodies (Active Motif, Carlsbad, CA). To ensure that equal amounts of SAGA containing and lacking Ubp8 were used in each experiment, each blot was then probed with anti-TAP antibodies (Open Biosystems, Huntsville, AL) to detect Ada2-CBP levels (see Fig. 4B and D, bottom panels).

**In vitro HAT assay.** Recombinant histone H3 (NEB, Ipswich, MA) was incubated for 1 h with SAGA complexes containing or lacking Ubp8 in histone acetyltransferase (HAT) buffer (50 mM Tris-HCl, pH 8.0, 10% glycerol, 0.1 mM EDTA, 1 mM DTT, 1 mM PMSF) containing [<sup>3</sup>H]acetyl coenzyme A ([<sup>3</sup>H]acetyl-CoA) at 37°C. Following the incubation, 5× SDS-PAGE loading buffer was added to each sample and samples were boiled at 95°C for 5 min. Samples were separated by SDS-PAGE and stained with Coomassie blue. Next, the gel was incubated with En<sup>3</sup>Hance (Perkin Elmer Life Sciences, Waltham, MA) for 1 h and washed with distilled water for 30 min. The gel was then dried overnight in a gel dryer on Whatman paper and exposed to autoradiograph film for 24 h to detect [<sup>3</sup>H]acetyl-histone H3 levels.

**Steady-state levels of *SNF1* mRNA.** Overnight cultures of BY4741 and yMW16 strains were diluted in 5 ml of YEP plus 2% glucose to a starting OD<sub>600</sub> of 0.2 and grown to a final OD<sub>600</sub> of 0.8 at 30°C. Cell pellets were collected from each sample and stored immediately on dry ice. Next, RNA was isolated from each sample by standard phenol-chloroform extraction procedures. Purified RNA was then subjected to either Northern blotting or quantitative reverse transcription-PCR (RT-PCR) methods.

**Stability of the Snf1-FLAG protein.** Overnight cultures of BY4741 and yMW16 strains containing pMW18 were diluted in 50 ml of SC-Leu plus 2% galactose and 2% sucrose to a starting OD<sub>600</sub> of 0.2 and grown to a final OD<sub>600</sub> of 0.8. At this point, cell pellets were collected by centrifugation and resuspended in 20 ml of SC-Leu without sugar. For time zero, a 1.5-ml aliquot was taken from each sample, and following centrifugation, the remaining cell pellet was immediately placed on dry ice. Next, transcription and translation were terminated by the addition of 4% glucose and 100 µg/ml of cycloheximide (Sigma, St. Louis, MO) to the media. Aliquots of each sample were taken at the indicated time points. Next, whole-cell extracts from each sample were analyzed by Western blotting with anti-FLAG antibodies (Sigma, St. Louis, MO) and anti-Pgk1 antibodies (Molecular Probes, Eugene, OR). Signals were quantified by using ImageQuant software.

In order to determine if the observed proteolysis in *ubp8Δ* strains was due to proteasome-mediated degradation of Snf1, the experiments were repeated as described above, except that 20 µM Z-Leu-Leu-Leu-al (MG132; Sigma, St. Louis, MO) was added at each step, starting with the media 2 h before time zero.

**Snf1 T210 phosphorylation measurements.** Overnight cultures of YSC1178-7500067 and yMW114 were diluted in 5 ml of the indicated media to a starting OD<sub>600</sub> of 0.2 and grown to a final OD<sub>600</sub> of 0.8 at 30°C. Cell pellets were collected by a 30-s centrifugation at 8,000 × g and quickly placed in liquid nitrogen. Cell extracts were then made by standard alkaline lysis and trichloroacetic acid (TCA) precipitation procedures with some modifications (26). Briefly, 2.7 × 10<sup>7</sup> cells were resuspended in 500 µl of cold double-distilled water (ddH<sub>2</sub>O). Eighty microliters of NaOH mix (1.85 M NaOH, 7.4% β-ME) was added to each tube, followed by incubation on ice for 10 min. Next, 80 µl of 50% TCA was added to each sample and incubated on ice for 10 min. Each sample was centrifuged for 4 min at 3,300 × g at 4°C. The supernatant was discarded and cell pellets were washed with 500 µl of 1 M Tris-HCl, pH 6.8. Sample pellets were collected and resuspended in 150 µl of 5× SDS-PAGE loading buffer. Samples were then separated by SDS-PAGE, transferred to nitrocellulose membranes, and probed with anti-protein A antibodies (Sigma, St. Louis, MO), anti-Pgk1 antibodies (Molecular Probes, Eugene, OR), or anti-phospho-Snf1 T210 antibodies (Cell Signaling, Danvers, MA).

**Gal83 phosphorylation measurements.** Overnight cultures of YSC1178-7500191, yMW129, and yMW134 grown in YEP plus 2% glucose were diluted in 100 ml of YEP plus 2% glucose to a starting OD<sub>600</sub> of 0.2 and grown to a final OD<sub>600</sub> of 0.7 at 30°C. Cell pellets were collected from each sample and washed in 50 ml of ddH<sub>2</sub>O and resuspended in 100 ml of YEP plus 2% glucose, YEP plus 2% galactose, or YEP plus 3% glycerol and 2% ethanol for 45 min. Cell pellets were then collected and frozen in liquid nitrogen. Whole-cell lysates were collected from each strain following resuspension of pellets in 1 ml of IP150 buffer (50 mM Tris-HCl, pH 7.5, 150 mM NaCl, 2 mM MgCl<sub>2</sub>, 0.1% Triton X-100, 10%

glycerol, 2× Complete protease inhibitors [Roche, Indianapolis, IN], 2× Phos-Stop phosphatase inhibitors [Roche, Indianapolis, IN]). Lysates were normalized and incubated for 3 h with 20 µl of pre-equilibrated IgG Sepharose (GE Healthcare, Piscataway, NJ) at 4°C and washed 3 times for 10 min each with IP150. Next, the beads were boiled in 5× SDS-PAGE loading buffer and eluates were separated by SDS-PAGE and transferred to a polyvinylidene difluoride (PVDF) membrane. Phospho-Gal83 was detected by staining the membrane with Pro-Q Diamond stain (Invitrogen, Carlsbad, CA). Briefly, the membrane was allowed to completely dry and then dipped in methanol. Next, the membrane was placed into a fix solution (7% acetic acid, 10% methanol) for 10 min and then washed 4 times with ddH<sub>2</sub>O for 5 min. The membrane was stained for 15 min with Pro-Q Diamond stain and destained with three 5-min washes in destain solution (50 mM sodium acetate [NaOAc], pH 4.0, 20% acetonitrile). The membrane was then dried and phospho-Gal83 was visualized on a Storm840 scanner. Total Gal83 was detected with an anti-protein A antibody (Sigma, St. Louis, MO) and visualized by using the Storm840 scanner.

## RESULTS

**The ubiquitination status of Snf1 is altered in the absence of Ubp8.** To identify potential Ubp8 substrates, we isolated ubiquitinated proteins from wild-type and *ubp8Δ* strains. Our reasoning was that ubiquitination of Ubp8 substrates would be increased in its absence, leading to an increased abundance of these proteins in ubiquitin isolations from *ubp8Δ* strains. The details of the isolation and a full list of potential targets identified by this screen will be presented elsewhere, but mass spectrometry of the isolated proteins identified Snf1 as a potential target of Ubp8. Snf1 was identified in two independent experiments, as was the known Ubp8 target, histone H2B (data not shown).

Snf1 is the founding member of the SNF1 family of AMP kinases (AMPKs), which is highly conserved from yeast to mammals (5, 10, 30). While it is involved in a wide variety of cellular processes, its major function in yeast is to induce expression of glucose-repressed genes when cells are grown on nonfermentable carbon sources through phosphorylation-mediated activation and deactivation of transcriptional regulators (28). To confirm the results of our biochemical screen, we purified 6×His-myc-ubiquitin from wild-type and *ubp8Δ* strains expressing a tandem affinity purification (TAP)-tagged version of Snf1 and a 6×His-myc epitope-tagged ubiquitin construct. After extensive washing, Ni-NTA-bound proteins were resolved by SDS-PAGE and analyzed by Western blot analyses with anti-TAP antibodies (Fig. 1A and B). We detected some ubiquitination of Snf1 in wild-type strains, but the abundance of the Snf1 ubiquitination was notably increased upon loss of Ubp8, further indicating that Snf1 is a target of Ubp8-mediated deubiquitination.

**Hyperubiquitination of Snf1 triggers proteasome-mediated degradation.** Ubiquitination of a protein can trigger its proteolysis. The isolations described above were performed in the presence of proteasome inhibitors in order to capture and enrich samples for ubiquitinated Ubp8 targets. To determine whether degradation of Snf1 is increased upon its hyperubiquitination, we determined whether steady-state levels of Snf1 were decreased in *ubp8Δ* strains. Importantly, we found that *SNF1* mRNA levels were unchanged in wild-type and *ubp8Δ* strains (Fig. 1C). Western blots, however, revealed that Snf1 protein levels decreased in the absence of Ubp8 (Fig. 2A and B).

To confirm that the decrease in Snf1 levels occurs posttranslationally, we monitored the stability of Snf1 expressed under



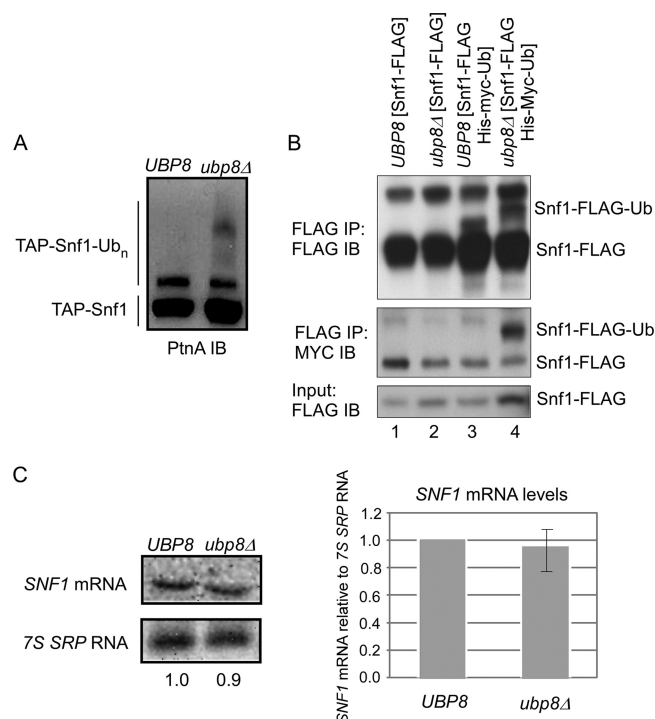


FIG. 1. In the absence of Ubp8, Snf1 becomes hyperubiquitinated. (A) Western blot analyses of Snf1 ubiquitination levels in the presence and absence of Ubp8. A 6×His pull-down of the 6×His-myc-ubiquitin reporter construct followed by an anti-PtnA Western blot analysis to detect Snf1. Left lane, wild-type (*UBP8*) yeast strains expressing 6×His-myc-ubiquitin; right lane, *ubp8Δ* strains expressing 6×His-myc-ubiquitin. IB, immunoblot. (B) A Snf1-FLAG immunoprecipitation (IP) in wild-type and *ubp8Δ* strains containing or lacking a His-myc-Ub reporter. (C) Northern blot (left) and quantitative RT-PCR (right;  $n = 3$ ) analyses of *SNF1* mRNA levels in wild-type and *ubp8Δ* strains.

the control of a galactose-inducible promoter at various time points following a shift of cells to repressing conditions (the addition of glucose) in the presence of cycloheximide, thus blocking transcription and translation of Snf1. Snf1 proteolysis occurred rapidly in *ubp8Δ* strains relative to wild-type strains (Fig. 2C and D). Further, this decrease in Snf1 stability was dependent on the carbon source, as it was observed only for *ubp8Δ* strains grown in galactose (Fig. 2E). Together, these data suggest that Ubp8 regulates Snf1 levels posttranslationally during growth on alternative carbon sources. In addition, the MG132 proteasome inhibitor stabilized Snf1 in *ubp8Δ* strains (*ubp8Δ* plus MG132; Fig. 2C and D), indicating that Ubp8-mediated deubiquitination protects Snf1 from proteasome-mediated degradation.

**Snf1 and Ubp8 are associated *in vivo*.** The finding that the ubiquitination status and stability of Snf1 are altered in *ubp8Δ* strains strongly suggests that Snf1 is a novel nonhistone substrate of Ubp8. If Ubp8 deubiquitinates Snf1, then we would expect to find interactions between these two proteins *in vivo*. To test this hypothesis, we coexpressed a FLAG epitope-tagged form of Snf1 and a myc epitope-tagged form of Ubp8 expressed from plasmid constructs. Western blots of anti-myc or anti-FLAG immunoprecipitates were probed with anti-FLAG or anti-myc antibodies to confirm that Snf1 and Ubp8 interact *in vivo* (Fig. 3A and B). In addition, we were still able

to detect these interactions in the presence of DNase and with the endogenously tagged proteins, indicating that the interactions are not mediated by DNA or are an artifact of the overexpression of these proteins, further supporting our hypothesis that Snf1 is a substrate of Ubp8 (Fig. 3A, B, and C).

**Ubp8 can deubiquitinate Snf1 *in vitro*.** To determine if Ubp8 can deubiquitinate Snf1 *in vitro*, we purified SAGA from strains that expressed a TAP-tagged version of Ada2, a component of the SAGA complex. In addition, we purified FLAG-tagged Snf1 from a strain that also expressed HA-tagged ubiquitin to be used as a substrate in these assays (Fig. 4C). For controls, in addition to purifying the known Ubp8 target, histone H2B, from a strain that also expressed HA-tagged ubiquitin (Fig. 4A), we performed an *in vitro* DUB assay with Ub-AMC (7-amino-4-methylcoumarin) to monitor the DUB activity of the purified complexes (Fig. 4F). Ubiquitinated Snf1 or H2B was incubated in the absence and presence of the SAGA complex and analyzed by use of anti-FLAG, anti-H2B, and anti-HA Western blots to determine whether SAGA could cleave ubiquitin from these proteins (Fig. 4B and D). SAGA cleaved ubiquitin from both histone H2B (Fig. 4B, lane 2) and Snf1 (Fig. 4D, lane 2). To confirm that the ability of SAGA to deubiquitinate Snf1 was specific to the activity of Ubp8, we also purified the SAGA complex from *ubp8Δ* strains. While the *in vitro* histone acetyltransferase activity of SAGA remained intact in the *ubp8Δ* strain (Fig. 4E, bottom panel, compare lanes 3 and 4), we observed a complete loss of SAGA-mediated deubiquitination of both histone H2B and Snf1, indicating that the observed deubiquitination described above was mediated by Ubp8 (Fig. 4B and D, lanes 3, and F). Together, these data indicate that Ubp8 can directly deubiquitinate Snf1.

**Snf1 hyperubiquitination corresponds to a decrease in Snf1 phosphorylation.** The activity of Snf1 and related AMP kinases is highly regulated (34). In mammals, AMPK acts as an energy sensor that becomes activated when cellular ratios of AMP to ATP are altered, which likely contributes to survival of a variety of tumors in nutrient-poor or hypoxic conditions. For example, for human glioblastoma multiform tumors, microenvironments of hypoxia that alter the energy balance of AMP and ATP result in increased expression of AMPK. Further, in glioma cell lines, hyperactive AMPK causes an increase in the expression of vascular endothelial growth factor (VEGF), a factor necessary for angiogenesis and survival of these high-grade tumors (25).

The activity of the Snf1 family is regulated in many different ways. One highly conserved mechanism involves the phosphorylation of the T loop at threonine 210 (T210) (14, 19, 24, 36), which closely parallels the activation of Snf1 and many other AMP kinases. When yeast cells grown in glucose are switched to less-preferred carbon sources, Snf1 becomes phosphorylated and then activates the expression of genes involved in utilization of these carbon sources by regulating the activity of downstream transcriptional modulators (12, 20, 28, 29, 33, 39). Interestingly, hyperubiquitination of mammalian Snf1-related AMP-activated protein kinases is associated with a marked decrease in T-loop phosphorylation, suggesting that ubiquitination regulates their activity (1).

To determine whether the hyperubiquitination of Snf1 that we observed for *ubp8Δ* strains affects its phosphorylation status, we monitored Snf1 T210 phosphorylation in wild-type and

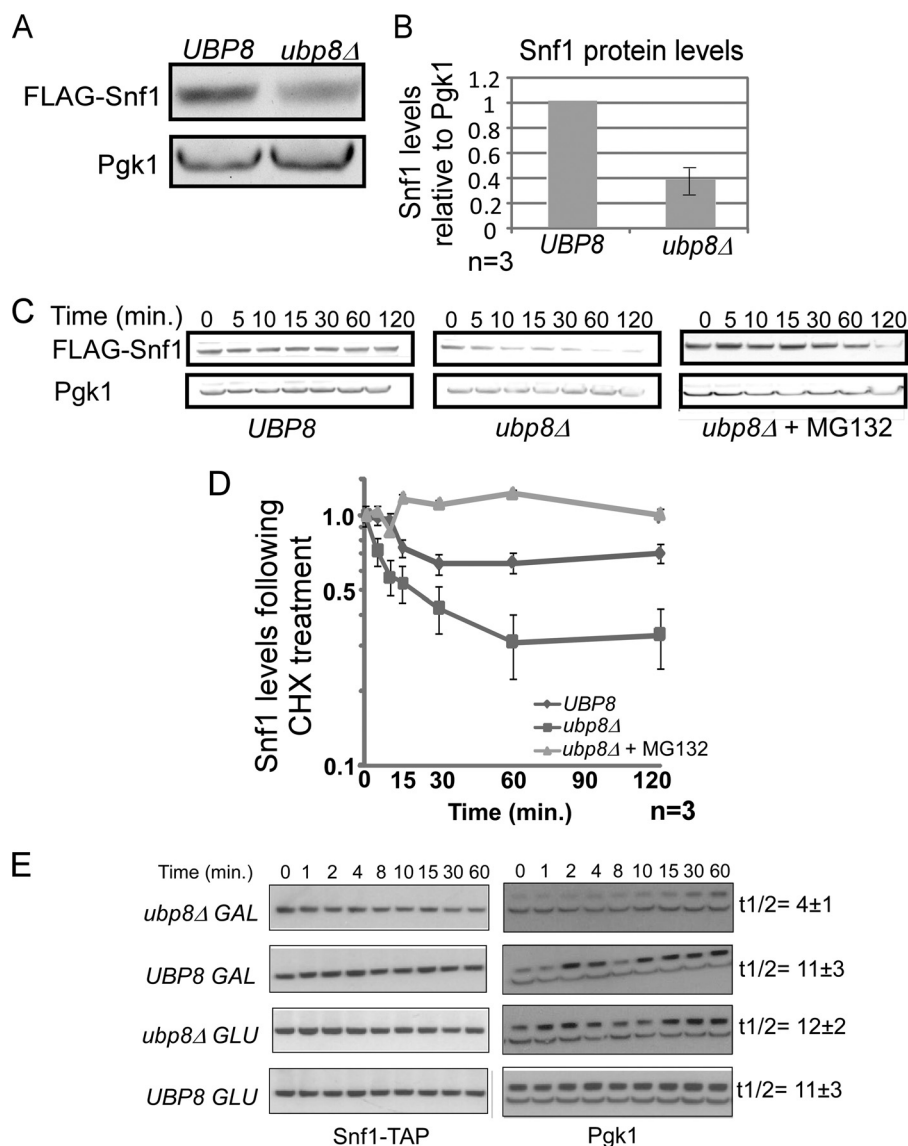


FIG. 2. The steady-state levels and stability of Snf1 are altered in *ubp8Δ* strains. (A) Western blot analysis of steady-state Snf1 levels in wild-type (*UB8*) and *ubp8Δ* strains. (B) Quantitation of Snf1 steady-state levels in *UB8* and *ubp8Δ* strains relative to the Pgk1 loading control was performed by densitometry analyses (ImageQuant) ( $n = 3$ ). (C) Western blot analyses of Snf1 stability in wild-type cells (left), *ubp8Δ* cells (middle), and *ubp8Δ* cells grown in the presence of the MG132 proteasome inhibitor (right). Strains were grown in galactose followed by a switch to growth in glucose and cycloheximide (CHX; 100  $\mu$ g/ml) to shut off transcription and translation of the *GAL-FLAG-SNF1* reporter. Snf1 levels were analyzed at the indicated time points in each strain by anti-FLAG Western blot analysis. (D) A quantitative analyses of Snf1 stability in each strain relative to Pgk1 was performed by densitometry analyses (ImageQuant) ( $n = 3$ ). (E) Western blot analyses of Snf1 stability of *ubp8Δ* cells and wild-type (*UB8*) cells grown in the presence of galactose (GAL) or glucose (GLU) relative to Pgk1. t1/2, half-life (in minutes).

*ubp8Δ* strains grown in activating (galactose) and nonactivating (glucose) carbon sources. Since Snf1 steady-state levels are decreased in *ubp8Δ* strains (Fig. 2A), we normalized the protein loads of Snf1 for these analyses. As expected, Snf1 T210 phosphorylation was regulated by the carbon source (Fig. 5B [top panel, compare lanes 1 and 3] and C), as it was increased in galactose-grown cells. In contrast, Snf1 T210 phosphorylation was reduced in *ubp8Δ* strains grown in galactose (Fig. 5B [compare lanes 3 and 4] and C), suggesting that, as for other AMP kinases, hyperubiquitination of Snf1 in the absence of Ubp8 affects T210 phosphorylation and potentially Snf1 activation.

**Snf1-mediated phosphorylation of Gal83 is decreased in *ubp8Δ* strains.** Decreased Snf1 T210 phosphorylation upon increased ubiquitination could lead to a decrease in Snf1 kinase activity. If so, then loss of Ubp8 might cause changes in gene expression similar to those caused by loss of Snf1. Therefore, we examined previously published microarray data and found significant overlaps between changes in gene expression reported for *snf1Δ* and *ubp8Δ* strains (16, 45). However, it is difficult to distinguish which changes are direct or indirect, as the SAGA complex and Snf1 each regulate many genes (Table 2). However, previously published chromatin immunoprecipitation microarray analysis (ChIP-chip) data revealed signifi-

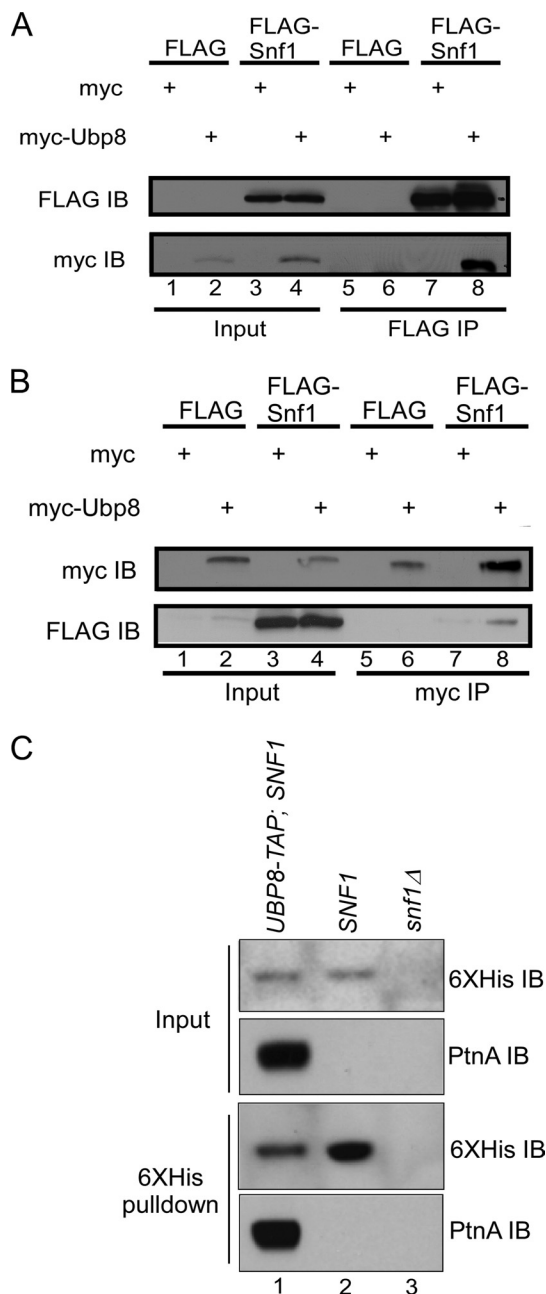


FIG. 3. Snf1 interacts with Ubp8 *in vivo*. (A and B) Whole-cell extracts were collected from yeast strains expressing an empty vector (lanes 1 and 5), Ubp8 with an N-terminal myc tag (lanes 2 and 6), or Snf1 with a C-terminal FLAG tag (lanes 3 and 7) or coexpressing both proteins (lanes 4 and 8). (A) Lysates were preincubated with 200 U of DNase for 1 h followed by incubation with anti-FLAG antibody-conjugated agarose beads. Each sample was analyzed by SDS-PAGE followed by anti-myc and anti-FLAG Western blot analyses. (B) Lysates from each sample were also incubated with anti-myc antibody-conjugated agarose beads. Each sample was analyzed by SDS-PAGE followed by anti-FLAG and anti-myc Western blot analyses. (C) Endogenously tagged Snf1 and Ubp8 interact *in vivo*. Whole-cell extracts were collected from yeast strains expressing either a TAP-tagged version of Ubp8 and Snf1, which has a natural stretch of histidine residues (lane 1), or Snf1 with untagged Ubp8 (lane 2) or lacking Snf1 and untagged Ubp8 (lane 3).

cant overlaps in Snf1 and Ubp8 binding at upstream activation sites (UAS) and transcriptional start sites (TSS) of many genes whose expression was affected by loss of these factors. This overlap in function at these genes supports the idea that Ubp8 modulates the activity of Snf1 to fine-tune the regulation of Snf1 target genes (Fig. 5A and Table 2) (16, 40, 45).

To more directly determine whether Snf1 activity is affected by Ubp8 loss, we examined the phosphorylation status of a Snf1 target protein. The Snf1 kinase complex is composed of a catalytic alpha subunit (Snf1), one of three beta subunits (Gal83, Sip1, and Sip2), and a gamma subunit (Snf4) (11). Each of the three beta subunits interacts with Snf1 and Snf4 to form three distinct isoforms of the Snf1 complex that have overlapping functions. Strains containing null mutations in any one of these proteins are viable on all carbon sources and show no differences in the phosphorylation status of downstream protein targets (32). Conversely, strains containing null mutations in all three of the beta subunits of the Snf1 complex phenocopy the growth and activity defects observed in *snf1* null mutants when grown on nonfermentable carbon sources (32). While the beta subunits appear to have shared functions, they can also confer substrate specificity to the Snf1 kinase complex, and they have distinct roles in the cell during growth on specific carbon sources (32).

The Snf1 complex containing the Gal83 beta subunit localizes to the nucleus during a switch from high- to low-glucose-containing media. Therefore, it is likely that this isoform of the Snf1 complex is posttranslationally modified by Ubp8. In addition, Gal83 is phosphorylated by Snf1 *in vivo* and *in vitro* (22, 41). Therefore, to determine if the hypophosphorylation of Snf1 that we observe in *ubp8Δ* strains corresponds to a decrease in Snf1 activity, we monitored the phosphorylation status of Gal83 in wild-type, *ubp8Δ*, and *snf1Δ* strains grown in activating (galactose) and nonactivating (glucose) carbon sources. Like Snf1 T210 phosphorylation, the phosphorylation of Gal83 is regulated by the carbon source (Fig. 5D, top panel, compare lanes 1 and 4), as it is phosphorylated when cells are grown in activating conditions. However, Gal83 phosphorylation is decreased in *ubp8Δ* strains (Fig. 5D, top panel, compare lanes 1 and 2), suggesting that the decrease in Snf1 stability and T210 phosphorylation that is observed in these strains corresponds to a decrease in Snf1 activity.

## DISCUSSION

One of the most studied modes of Snf1 regulation is the phosphorylation of threonine 210, a mark which closely follows Snf1 activation (14, 24, 36). In this study, we found that in addition to being modified by phosphorylation, Snf1 is modified by ubiquitination. Moreover, we discovered that Snf1 ubiquitination is regulated by the SAGA complex, as Snf1 becomes hyperubiquitinated in the absence of Ubp8 (Fig. 1 and 6). Snf1 physically interacts with Ubp8 *in vivo*, and the SAGA complex deubiquitinates Snf1 *in vitro*, in a Ubp8-dependent manner. To our knowledge, Snf1 is the first nonhistone substrate defined for the yeast DUB module of SAGA.

What is the biological function of Snf1 ubiquitination? One method to determine whether hyperubiquitination of Snf1 in *ubp8Δ* strains affects Snf1 activity is to determine whether *snf1Δ* and *ubp8Δ* strains share growth defects. However, one

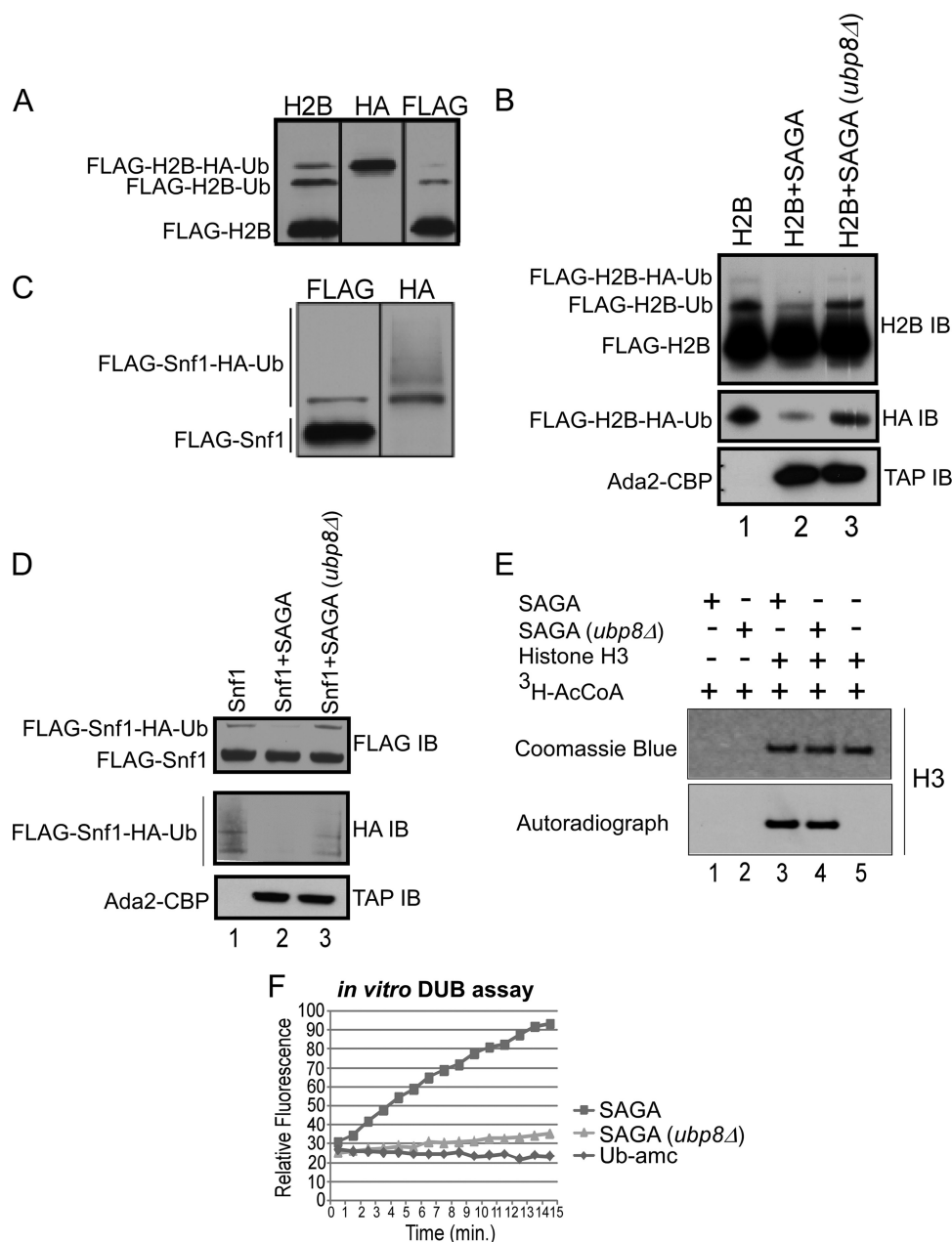


FIG. 4. SAGA deubiquitinates Snf1 *in vitro*. (A) Ubiquitinated histone H2B was purified in strains expressing a FLAG epitope-tagged H2B and a 3×HA epitope-tagged ubiquitin. Ubiquitination of purified H2B was confirmed by Western blotting with anti-H2B, anti-HA, and anti-FLAG antibodies. (B) To confirm that SAGA directly deubiquitinates histone H2B *in vitro*, purified H2B was incubated in the absence (lane 1) and presence of SAGA complexes that contained (lane 2) or lacked (lane 3) Ubp8. The ubiquitination status of H2B was monitored by Western blot analyses with anti-H2B (top panel) and anti-HA (middle panel) antibodies. (C) Ubiquitinated Snf1 was purified from strains expressing a FLAG-epitope tagged Snf1 and a 3×HA epitope-tagged ubiquitin. Ubiquitination of the purified Snf1 was confirmed by Western blot analysis with anti-FLAG and anti-HA antibodies. (D) Purified Snf1 was incubated in the absence (lane 1) or presence of SAGA complexes that contained (lane 2) or lacked (lane 3) the deubiquitination module. The ubiquitination status of Snf1 was monitored by Western blot analyses with anti-FLAG (top panel) and anti-HA (middle panel) antibodies. (E) An *in vitro* histone acetyltransferase assay to determine the activity of SAGA complexes containing (lane 3) and lacking (lane 4) Ubp8. <sup>3</sup>H-AcCoA, [<sup>3</sup>H]acetyl-CoA. (F) An *in vitro* deubiquitination (DUB) assay to determine the DUB activity of SAGA complexes containing (SAGA) and lacking (SAGA *ubp8Δ*) Ubp8 toward the fluorogenic substrate, ubiquitin-AMC (Ub-amc), as measured by fluorescence over time.

problem with testing this hypothesis is that *ubp8Δ* strains, unlike *snf1Δ* strains, have growth defects on preferred (control) carbon sources (i.e., glucose [data not shown]), which makes interpretation of any results difficult. However, our data indi-

cate that Ubp8 does in fact regulate Snf1, as it regulates both the half-life of Snf1 and its kinase activity. Interestingly, while ubiquitination of other AMP kinases (AMPKs) has been described, only a few studies address the regulation of these



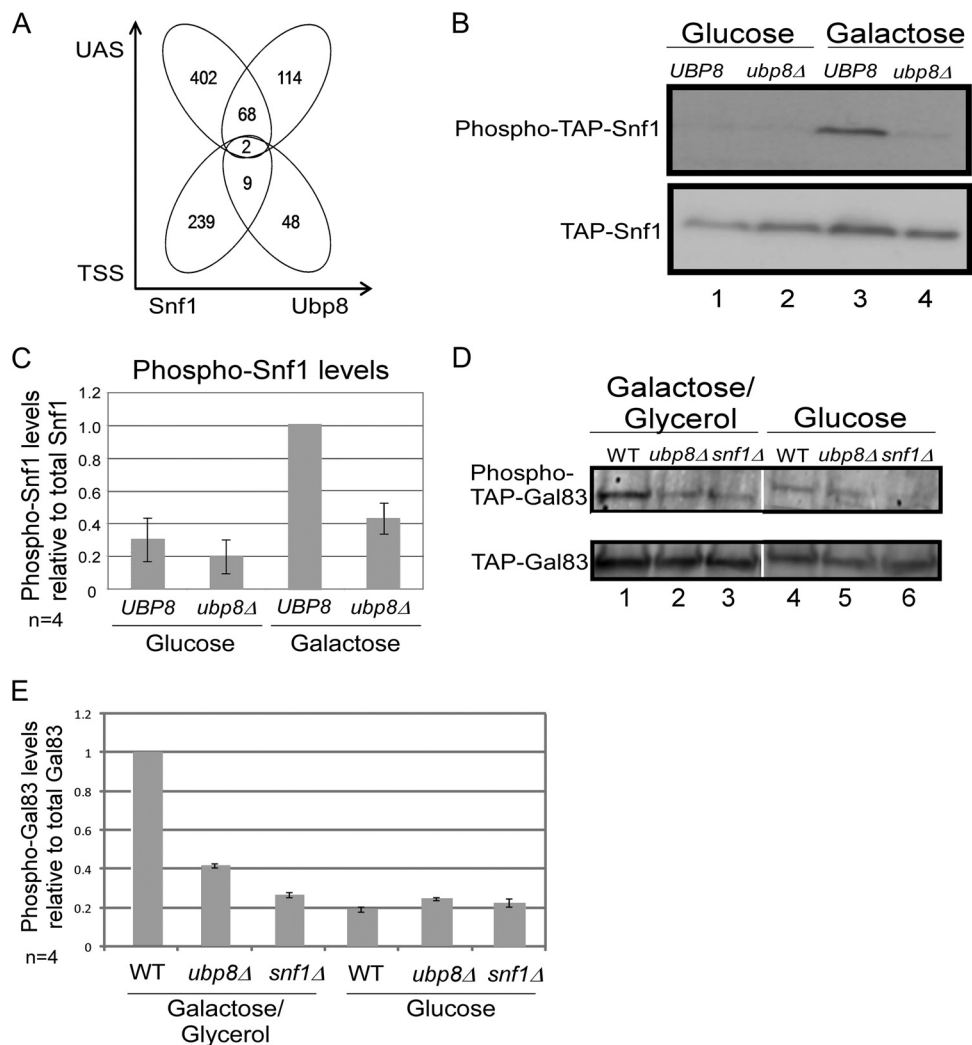


FIG. 5. Hyperubiquitination of Snf1 fine-tunes its activity. (A) A graphical representation of Table 2, presenting Snf1 and Ubp8 ChIP-chip data that were used in a comparative BLAST search in order to determine overlaps between Snf1 and Ubp8 binding sites (x axis) at the upstream activation sites (UAS) and transcriptional start sites (TSS) of the indicated genes (y axis). Numbers represent numbers of genes. (B) Wild-type (*UBP8*) and *ubp8Δ* cells expressing TAP-tagged Snf1 were lysed by alkaline lysis to monitor the phosphorylation status of Snf1 when cells were grown in activating (galactose) or nonactivating (glucose) medium. To account for the decrease in steady-state levels of Snf1 in *ubp8Δ* strains that we observed earlier, we loaded 3-fold more *ubp8Δ* lysates than wild-type lysates (lanes 2 and 4) into the lanes to normalize Snf1 between strains. Snf1 T210 phosphorylation was monitored in each strain by Western blotting with anti-TAP and anti-phospho-Snf1 T210 antibodies. (C) Phospho-Snf1 levels in *UBP8* and *ubp8Δ* cells were measured relative to total Snf1 levels by using densitometry analyses (ImageQuant) (*n* = 4). (D) Snf1 activity was monitored by measuring the phosphorylation status of Gal83. (Upper panel) Phospho-TAP-Gal83 staining; (lower panel) TAP-Gal83 Western blot. WT, wild type. (E) Phospho-Gal83 levels in WT, *ubp8Δ*, and *snf1Δ* strains were measured relative to total Gal83 by using densitometry analyses (ImageQuant) (*n* = 4).

enzymes by ubiquitination. The mammalian USP9X deubiquitinase regulates the ubiquitination status of the MARK4 and NUA1 AMPK-related kinases (1). Similar to what was seen in our findings, MARK4 and NUA1 are hyperubiquitinated in the absence of USP9X. However, hyperubiquitination of these enzymes does not seem to affect their stability but rather has a negative effect on MARK4 and NUA1 T-loop phosphorylation. Since ubiquitination of Snf1 not only affected its stability, but like MARK4 and NUA1, also had a negative effect on its phosphorylation status, the activity of Snf1 is likely tightly regulated by the opposing actions of Ubp8 and ubiquitin ligases. In yeast and mammals, the major upstream activating kinases of the SNF1 family of proteins (in yeast, Sak1, Tos3,

and Elm1, and in mammals, LKB1 and CaMKK) are constitutively active (15). However, when cells are grown in activating conditions, only a fraction of these kinase targets is phosphorylated. Therefore, it is possible that in a system that is “always on,” the ubiquitination/deubiquitination cycles of SNF1 family members have evolved to allow only a portion of each family member to be recognized by or accessible to these upstream kinases. Similarly, Ubp8-mediated deubiquitination of Snf1 may have evolved to fine-tune the spatial and temporal activation of Snf1.

Snf1 can directly phosphorylate histone proteins, transcriptional modulators, and the beta subunits of the Snf1 kinase complex isoforms. Mutations that inactivate Snf1 cause a de-



TABLE 2. ChIP-chip/microarray data intersections

Gene name	ChIP-chip binding of:		Microarray <sup>a</sup>		Gene name	ChIP-chip binding:		Microarray	
	Snf1-TAP	Ubp8-TAP	<i>snf1</i>	<i>ubp8</i>		Snf1-TAP	Ubp8-TAP	<i>snf1</i>	<i>ubp8</i>
UAS intersection					<i>YLR270W/DCS1</i>	1.4	1.97		0.027567
<i>YCR008W/SAT4</i>	2.67	1.57		−0.06098	<i>YLR401C/DUS3</i>	1.97	1.5		−0.03535
<i>YCR066W/RAD18</i>	1.31	1.18		0.03486	<i>YLR438W/CAR2</i>	1.02	2.5	0.434	−0.00273
<i>YCR094W/CDC50</i>	2.68	2.41		−0.00221	<i>YMR010W</i>	1.74	2.08	−0.28	0.014928
<i>YDL021W/GPM2</i>	1.55	1.1		−0.0994	<i>YMR012W/CLU1</i>	1.15	1.01	−0.168	−0.05255
<i>YDL045W_A/MRP10</i>	1.44	1.05		−0.07186	<i>YMR234W/RNH1</i>	2.59	2.48		0.074478
<i>YDL058W/MRP10</i>	1.65	1.87		0.04083	<i>YMR262W</i>	2.37	1.72		0.031968
<i>YDR192C/NUP42</i>	1.34	1.17		−0.01565	<i>YNL004W/HRB1</i>	1.84	2.02		−0.11802
<i>YDR260C/SWM1</i>	1.43	1.54		−0.03153	<i>YNL279W/PRM1</i>	2.06	2.56		
<i>YDR316W-B</i>	1.16	1.24		−0.04028	<i>YNR022C/MRPL50</i>	1.22	1.34	−0.12	−0.01336
<i>YDR358W/GGA1</i>	3.13	2.66		−0.12448	<i>YOL020W/TAT2</i>	1.12	1.66	−0.388	0.026485
<i>YDR514C</i>	2.59	2.72		−0.02023	<i>YOR036W/PEP12</i>	1.03	1.13		0.098957
<i>YER039C-A</i>	1.64	1.63		−0.02868	<i>YOR044W/IRC23</i>	1.33	1.47		−0.11018
<i>YER057C/HIG1</i>	1.11	1.54	0.083	−0.0386	<i>YOR100C/CRC1</i>	1.97	2.86	0.749	0.065734
<i>YER090W/TRP2</i>	1.05	1.28	−0.301	−0.04919	<i>YOR230W/WTM1</i>	2.93	2.55		0.051374
<i>YER091C/MET6</i>	1.42	1.23	0.175	0.057372	<i>YPL016W/SWI1</i>	2.53	3.02		−0.03849
<i>YER103W/SSA4</i>	1.03	1.39		−0.09116	<i>YPL033C/SRL4</i>	2.56	2	−0.537	−0.01147
<i>YER106W/MAM1</i>	1.11	1.39	0.224	−0.02062	<i>YPL058C/PDR12</i>	2.46	2.34		0.03959
<i>YER146W/LSM5</i>	1.12	1.67		−0.01246	<i>YPL104W/MSD1</i>	1.37	1.17	0.113	−0.05319
<i>YER151C/UBP3</i>	1.75	1.72		−0.03038	<i>YPL135W/ISU1</i>	1.64	1.66	−0.096	−0.09092
<i>YER182W/FMP10</i>	1.14	1.48	−0.316	−0.00777	<i>YPL180W/TOR89</i>	1.62	2.41		−0.00119
<i>YGL138C</i>	2.49	2.96	0.505	−0.14168	<i>YPL208W/RKM1</i>	1.08	1.1		−0.01421
<i>YGL168W/HUR1</i>	2.2	2.78		0.039632	<i>YPL216W</i>	1.38	1.76		0.011825
<i>YGR154C/GTO1</i>	2.25	1.62		−0.03293	<i>YPL220W/RPL1A</i>	1.85	2.25		−0.01482
<i>YHL026C</i>	2.48	3.17		0.000116	<i>YPL231W/FAS2</i>	3.18	3.08		
<i>YHR005C/GTA1</i>	2.74	2.62		−0.04459	<i>YPR086W/SUA7</i>	1.43	1.83		−0.06619
<i>YHR042W/NCP1</i>	1.09	1.22		−0.00386	<i>YPR108W-A</i>	2.53	1.91		
<i>YHR176W/FMO1</i>	1.46	1.14		0.12725	TSS intersection				
<i>YHR178W/STB5</i>	1.07	1.37		0.009928	<i>YAR019C/CDC15</i>	2.55	1.54		−0.01449
<i>YHR187W/IKI1</i>	2.89	1.95		−0.01426	<i>YDL045W_A/MRP10</i>	1.27	1.14		−0.07186
<i>YIL046W-A</i>	2.29	2.1			<i>YDL052C/SLC1</i>	1.15	1.05	−0.16	
<i>YIL091C/UTP25</i>	1.18	1.44		−0.11593	<i>YDR358W/GGA1</i>	1.34	1.34		−0.12448
<i>YJL073W/JEM1</i>	1.29	1.25	−0.173	−0.08061	<i>YKL095W/YJU2</i>	1.25	1.34		0.074038
<i>YKL061W/BLI1</i>	3.14	3.07		0.018122	<i>YKR045C</i>	1.78	1.56		0.053793
<i>YKL112W/BAF1</i>	2.35	2.26		−0.05439	<i>YML094W/GIM5</i>	1.98	2.68		0.027821
<i>YKL161C/KDX1</i>	1.29	1.39	−0.407	0.039902	<i>YNR057C/BIO4</i>	1.57	2.02	−0.185	0.11259
<i>YKR024C/DPB7</i>	1.1	1.06	−0.193	−0.02473	<i>YPL245W</i>	2.44	1.35		0.024861
<i>YKR090W/PXL1</i>	1.87	2.47		−0.12053	UAS/TSS intersection				
<i>YLR057W/MNL2</i>	3.26	3.16		−0.01818	<i>YDL045W_A/MRP10</i>	1.27	1.14		−0.0718
<i>YLR095C/IOC2</i>	1.31	1.02		0.046575	<i>YDR358W/GGA1</i>	1.34	1.34		−0.1244
<i>YLR154C-G</i>	1.3	1.99							
<i>YLR187W/SKG3</i>	2.28	1.35	0.332	−0.10784					

<sup>a</sup> Values are changes in gene expression.

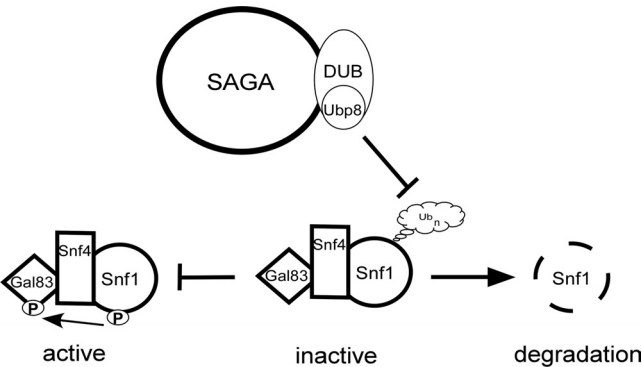


FIG. 6. Model of Ubp8-mediated regulation of Snf1. Model of how Ubp8 and ubiquitination of Snf1 control Snf1 levels and kinase activity. The SAGA complex (through the DUB module) deubiquitinates and protects Snf1 from proteasome-mediated degradation. In addition, Ubp8-mediated deubiquitination of Snf1 promotes Snf1 activation on nonpreferred carbon sources and subsequent Snf1-mediated phosphorylation of specific downstream protein targets.

crease in the phosphorylation of these downstream targets (22, 41). We show that SAGA, through the Ubp8 deubiquitinase, fine-tunes these activities, as hyperubiquitination of Snf1 decreases phosphorylation of both Snf1 and its downstream target, Gal83. Therefore, Ubp8 functions positively reinforce Snf1-mediated activities in the cell (Fig. 6).

Our data not only provide additional information about the molecular mechanisms of the SAGA complex but also suggest that ubiquitination of AMPKs provides a mechanism that is conserved from yeast to humans for the regulation of their activity. Future work will identify the ubiquitin ligase that is responsible for Snf1 ubiquitination and the mechanism by which Snf1 ubiquitination inhibits its activation.

Our current and previous works demonstrate that SAGA utilizes multiple mechanisms to fine-tune gene expression beyond chromatin structure. Therefore, like for the Snf1 AMPK, the identification and characterization of these additional targets of the SAGA complex will be critical to

understanding the role that USP22 and SAGA play in the death-from-cancer signature that is observed in various carcinomas (7, 8).

### ACKNOWLEDGMENTS

We thank William Dubinsky (The University of Texas Dental Branch) for performing the mass spectrometry experiments. We thank Ambro van Hoof, Daneen Grossman, Kevin Morano, and Hugo Tapia (The University of Texas Health Science Center at Houston), Hugo Bellen and Nikos Giagtzoglou (Baylor College of Medicine), and Jerry Workman and Kenneth Lee (Stowers Institute) for yeast strains, reagents, and equipment that were used to conduct this work. We also thank Daniel Finley (Harvard Medical School) and Richard Gardner (University of Washington) for generously sharing plasmids. We thank Ambro van Hoof, John Latham, Yi Chun Chen, Jill Butler, Boyko Atanassov, and Marek Napierela (The University of Texas M. D. Anderson Cancer Center) for fruitful discussions.

This work was supported by the National Institute of Child Health and Human Development Training Grant in "Differentiation and Development" to M.A.W. (2 T32 HD07325) and grants from the NIH (R01GM51189) and the MDACC Senior Research Trust to S.Y.R.D.

### REFERENCES

- Al-Hakim, A. K., et al. 2008. Control of AMPK-related kinases by USP9X and atypical Lys(29)/Lys(33)-linked polyubiquitin chains. *Biochem. J.* **411**: 249–260.
- Atanassov, B. S., et al. 2009. Gcn5 and SAGA regulate shelterin protein turnover and telomere maintenance. *Mol. Cell* **35**:352–364.
- Burrows, J. F., et al. 2009. USP17 regulates Ras activation and cell proliferation by blocking RCE1 activity. *J. Biol. Chem.* **284**:9587–9595.
- Daniel, J. A., and P. A. Grant. 2007. Multi-tasking on chromatin with the SAGA coactivator complexes. *Mutat. Res.* **618**:135–148.
- Daniel, T., and D. Carling. 2002. Expression and regulation of the AMP-activated protein kinase-Snf1 (sucrose non-fermenting 1) kinase complexes in yeast and mammalian cells: studies using chimaeric catalytic subunits. *Biochem. J.* **365**:629–638.
- Gietz, R. D., and R. A. Woods. 2002. Transformation of yeast by lithium acetate/single-stranded carrier DNA/polyethylene glycol method. *Methods Enzymol.* **350**:87–96.
- Glinisky, G. V. 2005. Death-from-cancer signatures and stem cell contribution to metastatic cancer. *Cell Cycle* **4**:1171–1175.
- Glinisky, G. V. 2006. Genomic models of metastatic cancer: functional analysis of death-from-cancer signature genes reveals aneuploid, aneuploid-resistant, metastasis-enabling phenotype with altered cell cycle control and activated Polycomb Group (PcG) protein chromatin silencing pathway. *Cell Cycle* **5**:1208–1216.
- Grant, P. A., D. E. Sterner, L. J. Duggan, J. L. Workman, and S. L. Berger. 1998. The SAGA unfolds: convergence of transcription regulators in chromatin-modifying complexes. *Trends Cell Biol.* **8**:193–197.
- Hardie, D. G., D. Carling, and M. Carlson. 1998. The AMP-activated/Snf1 protein kinase subfamily: metabolic sensors of the eukaryotic cell? *Annu. Rev. Biochem.* **67**:821–855.
- Hedbacker, K., and M. Carlson. 2008. Snf1/AMPK pathways in yeast. *Front. Biosci.* **13**:2408–2420.
- Hedges, D., M. Proft, and K. D. Entian. 1995. CAT8, a new zinc cluster-encoding gene necessary for derepression of gluconeogenic enzymes in the yeast *Saccharomyces cerevisiae*. *Mol. Cell. Biol.* **15**:1915–1922.
- Henry, K. W., et al. 2003. Transcriptional activation via sequential histone H2B ubiquitylation and deubiquitylation, mediated by SAGA-associated Ubp8. *Genes Dev.* **17**:2648–2663.
- Hong, S. P., F. C. Leiper, A. Woods, D. Carling, and M. Carlson. 2003. Activation of yeast Snf1 and mammalian AMP-activated protein kinase by upstream kinases. *Proc. Natl. Acad. Sci. U. S. A.* **100**:8839–8843.
- Hong, S. P., M. Momcilovic, and M. Carlson. 2005. Function of mammalian LKB1 and Ca2+/calmodulin-dependent protein kinase alpha as Snf1-activating kinases in yeast. *J. Biol. Chem.* **280**:21804–21809.
- Ingvarsdottir, K., et al. 2005. H2B ubiquitin protease Ubp8 and Sgf11 constitute a discrete functional module within the *Saccharomyces cerevisiae* SAGA complex. *Mol. Cell. Biol.* **25**:1162–1172.
- Koutelou, E., C. L. Hirsch, and S. Y. Dent. 2010. Multiple faces of the SAGA complex. *Curr. Opin. Cell Biol.* **22**:374–382.
- Lee, K. K., L. Florens, S. K. Swanson, M. P. Washburn, and J. L. Workman. 2005. The deubiquitylation activity of Ubp8 is dependent upon Sgf11 and its association with the SAGA complex. *Mol. Cell. Biol.* **25**:1173–1182.
- Leech, A., N. Nath, R. R. McCartney, and M. C. Schmidt. 2003. Isolation of mutations in the catalytic domain of the snf1 kinase that render its activity independent of the snf4 subunit. *Eukaryot. Cell* **2**:265–273.
- Lesage, P., X. Yang, and M. Carlson. 1996. Yeast SNF1 protein kinase interacts with SIP4, a C6 zinc cluster transcriptional activator: a new role for SNF1 in the glucose response. *Mol. Cell. Biol.* **16**:1921–1928.
- Machida, Y. J., Y. Machida, A. A. Vashisht, J. A. Wohlschlegel, and A. Dutta. 2009. The deubiquitinating enzyme BAP1 regulates cell growth via interaction with HCF-1. *J. Biol. Chem.* **284**:34179–34188.
- Mangat, S., D. Chandrashekarappa, R. R. McCartney, K. Elbing, and M. C. Schmidt. 2010. Differential roles of the glycogen-binding domains of beta subunits in regulation of the Snf1 kinase complex. *Eukaryot. Cell* **9**:173–183.
- Martinez, E. 2002. Multi-protein complexes in eukaryotic gene transcription. *Plant Mol. Biol.* **50**:925–947.
- Nath, N., R. R. McCartney, and M. C. Schmidt. 2003. Yeast Pak1 kinase associates with and activates Snf1. *Mol. Cell. Biol.* **23**:3909–3917.
- Neurath, K. M., M. P. Keough, T. Mikkelsen, and K. P. Claffey. 2006. AMP-dependent protein kinase alpha 2 isoform promotes hypoxia-induced VEGF expression in human glioblastoma. *Glia* **53**:733–743.
- Ooi, C. E., E. Rabinovich, A. Dancis, J. S. Bonifacio, and R. D. Klausner. 1996. Copper-dependent degradation of the *Saccharomyces cerevisiae* plasma membrane copper transporter Ctr1p in the apparent absence of endocytosis. *EMBO J.* **15**:3515–3523.
- Pereg, Y., et al. 2010. Ubiquitin hydrolase Dub3 promotes oncogenic transformation by stabilizing Cdc25A. *Nat. Cell Biol.* **12**:400–406.
- Rahner, A., A. Scholer, E. Martens, B. Gollwitzer, and H. J. Schuller. 1996. Dual influence of the yeast Cat1p (Snf1p) protein kinase on carbon source-dependent transcriptional activation of gluconeogenic genes by the regulatory gene CAT8. *Nucleic Acids Res.* **24**:2331–2337.
- Randez-Gil, F., N. Bojunga, M. Proft, and K. D. Entian. 1997. Glucose derepression of gluconeogenic enzymes in *Saccharomyces cerevisiae* correlates with phosphorylation of the gene activator Cat8p. *Mol. Cell. Biol.* **17**:2502–2510.
- Sanz, P. 2003. Snf1 protein kinase: a key player in the response to cellular stress in yeast. *Biochem. Soc. Trans.* **31**:178–181.
- Sasaki, H., et al. 2001. Expression of the protein gene product 9.5, PGP9.5, is correlated with T-status in non-small cell lung cancer. *Jpn. J. Clin. Oncol.* **31**:532–535.
- Schmidt, M. C., and R. R. McCartney. 2000. Beta-subunits of Snf1 kinase are required for kinase function and substrate definition. *EMBO J.* **19**:4936–4943.
- Smith, F. C., S. P. Davies, W. A. Wilson, D. Carling, and D. G. Hardie. 1999. The SNF1 kinase complex from *Saccharomyces cerevisiae* phosphorylates the transcriptional repressor protein Mig1p in vitro at four sites within or near regulatory domain 1. *FEBS Lett.* **453**:219–223.
- Steinberg, G. R., and B. E. Kemp. 2009. AMPK in health and disease. *Physiol. Rev.* **89**:1025–1078.
- Sterner, D. E., et al. 1999. Functional organization of the yeast SAGA complex: distinct components involved in structural integrity, nucleosome acetylation, and TATA-binding protein interaction. *Mol. Cell. Biol.* **19**:86–98.
- Sutherland, C. M., et al. 2003. Elm1p is one of three upstream kinases for the *Saccharomyces cerevisiae* SNF1 complex. *Curr. Biol.* **13**:1299–1305.
- Tansey, W. 2006. Detection of ubiquitylated proteins in yeast. Cold Spring Harbor Laboratory Press, Cold Spring Harbor, NY.
- Tezel, E., K. Hibi, T. Nagasaka, and A. Nakao. 2000. PGP9.5 as a prognostic factor in pancreatic cancer. *Clin. Cancer Res.* **6**:4764–4767.
- Treitel, M. A., S. Kuchin, and M. Carlson. 1998. Snf1 protein kinase regulates phosphorylation of the Mig1 repressor in *Saccharomyces cerevisiae*. *Mol. Cell. Biol.* **18**:6273–6280.
- Venters, B. J., et al. 2011. A comprehensive genomic binding map of gene and chromatin regulatory proteins in *Saccharomyces*. *Mol. Cell* **41**:480–492.
- Vincent, O., R. Townley, S. Kuchin, and M. Carlson. 2001. Subcellular localization of the Snf1 kinase is regulated by specific beta subunits and a novel glucose signaling mechanism. *Genes Dev.* **15**:1104–1114.
- Woods, R. A., and R. D. Gietz. 2001. High-efficiency transformation of plasmid DNA into yeast. *Methods Mol. Biol.* **177**:85–97.
- Wyce, A., et al. 2007. H2B ubiquitylation acts as a barrier to Ctk1 nucleosomal recruitment prior to removal by Ubp8 within a SAGA-related complex. *Mol. Cell* **27**:275–288.
- Yaglom, J., et al. 1995. p34Cdc28-mediated control of Cln3 cyclin degradation. *Mol. Cell. Biol.* **15**:731–741.
- Young, E. T., K. M. Dombek, C. Tachibana, and T. Ideker. 2003. Multiple pathways are co-regulated by the protein kinase Snf1 and the transcription factors Adr1 and Cat8. *J. Biol. Chem.* **278**:26146–26158.
- Yuan, J., K. Luo, L. Zhang, J. C. Cheville, and Z. Lou. 2010. USP10 regulates p53 localization and stability by deubiquitinating p53. *Cell* **140**:384–396.
- Zhao, Y., et al. 2008. A TFTC/STAGA module mediates histone H2A and H2B deubiquitination, coactivates nuclear receptors, and counteracts heterochromatin silencing. *Mol. Cell* **29**:92–101.